

# Two conductivity regimes in semiconductor $\delta$ -layer tunnel junctions

D. Mamaluy<sup>1</sup>, and J.P. Mendez<sup>1</sup>

<sup>1</sup>Cognitive & Emerging Computing, Sandia National Laboratories, Albuquerque, USA

[mamaluy@sandia.gov](mailto:mamaluy@sandia.gov)

We present an open-system quantum-mechanical charge self-consistent 3D real-space study of the conduction band structure and conductive properties of phosphorus delta-layer tunnel junctions in silicon shown in Fig. 1. These structures serve as basic building blocks for beyond-Moore (classical digital) (e.g. [1]) and quantum computing applications (e.g. [2]). Recent high resolution ARPES experiments [3, 4] demonstrated that the traditional band structure calculation methods that are based on either periodic or Dirichlet boundary conditions fail to describe the existence of  $3\Gamma$  subband without adjusting the dielectric constant of Si to 40. Recently we demonstrated that using the open system boundary conditions (for the charge self-consistent Schrodinger equation) that preserve the quantum-mechanical flux allows to explain the existence of  $3\Gamma$  subband without any fitting parameters and accurately reproduce the sheet resistance values for a wide range of delta-layer doping densities and different experimental groups [5]. Here we extend the open-system charge self-consistent quantum transport analysis to delta-layer tunnel junctions. The performed numerical analysis predicts that *the strong conduction band quantization leads to the existence of two distinct Ohmic conductivity regimes* as shown in Fig. 2. The corresponding mechanism can be understood from Figure 3, where the computed local

density of states is shown. For cryogenic temperatures only the states below Fermi level are occupied. As can be seen from Figure 3, the strong delta-layer confinement leads to the *conduction band quantization*. For low voltages, there is a mismatch between the quasi-discrete states on the left that have to tunnel to the quasi-discrete states on the right side, which reduces the conductivity. For higher applied drain voltages, the quasi-continuum states on the right side become available to tunnel into from the left side that eliminates the mis-match and increases conductivity [6]. Recent experimental data [2] for the I-V characteristics in Si:P delta-layer tunnel junctions support the existence of the two conductivity regimes. The “threshold” voltage (around 0.05-0.07 V in Fig. 2) is a function of doping level and doping thickness, and could be controlled for device applications.

## REFERENCES

- [1] He, Y. et al., Nature 571, 371–375 (2019).
- [2] M. B. Donnelly, J. G. Keizer, Y. Chung, and M. Y. Simmons, Nano Letters 21, 10092 (2021).
- [3] A. J. Holt et al., Phys. Rev. B 101, 121402 (2020).
- [4] F. Mazzola, CY. Chen, R. Rahman et al., npj Quantum Mater. 5, 34 (2020).
- [5] D. Mamaluy, J.P. Mendez, X. Gao, et al. Commun Phys 4, 205 (2021).
- [6] J.P.Mendez, D. Mamaluy, Sci Rep 12, 16397 (2022).

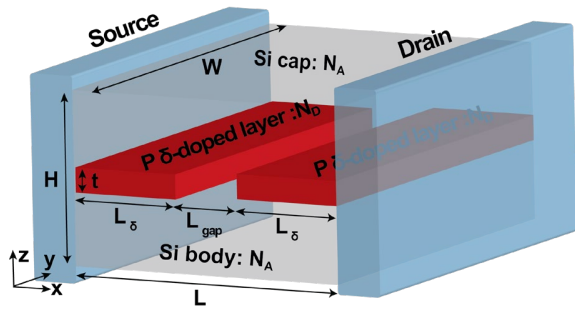


Fig.1: Ideal Si:P  $\delta$ -layer tunnel junction (TJ) devices. The ideal device consists of a semi-infinite source and drain, in contact with the channel. The channel is composed of a lightly doped Si body and Si cap and a very thin, highly P doped-layer with an intrinsic gap of length  $L_{\text{gap}}$ .

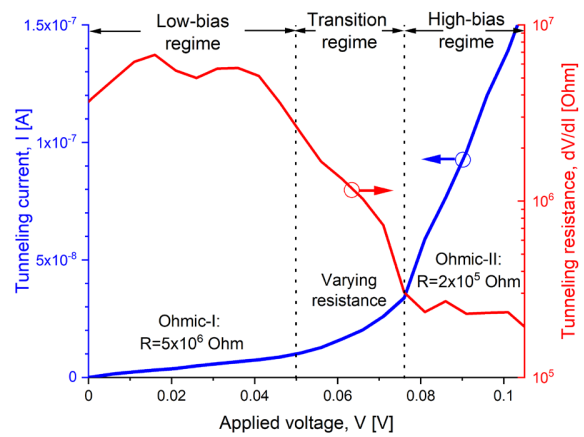


Fig.2: Two conductivity regimes in  $\delta$ -layer tunnel junctions. Total current vs voltage (blue curve, linear scale) and the corresponding differential resistance  $dV/dI$  (red curve, logarithmic scale) are shown for  $L_{\text{gap}}=10\text{nm}$ ,  $N_D=1.0 \times 10^{14}\text{cm}^{-2}$ ,  $N_A=5.0 \times 10^{17}\text{cm}^{-3}$  and  $t=1\text{nm}$ .

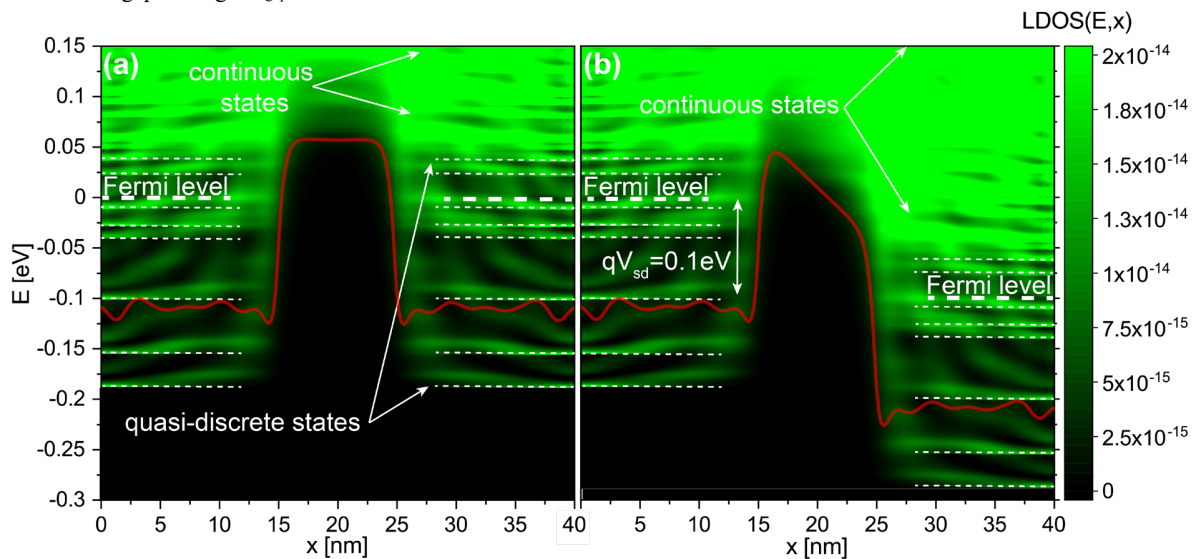


Fig.3: Local Density of States for  $\delta$ -layer tunnel junctions. The LDOS( $E,x$ ) for a tunnel junction of  $L_{\text{gap}}=10\text{nm}$  is shown in (a) and (b) when a voltage of 1 mV and 100 mV is applied to the drain contact, respectively. The Fermi levels indicated in the figures correspond to the Fermi levels of the source and drain contacts. In (a) and (b), the corresponding effective 1D potentials are also shown, calculated by integrating over the ( $y,z$ )-plane the actual charge self-consistent 3D potentials weighted with the electron density.  $N_D=1.0 \times 10^{14}\text{cm}^{-2}$ ,  $N_A=5.0 \times 10^{17}\text{cm}^{-3}$ , and  $t=1\text{nm}$ .